

Marc Libault · Federico Tessadori · Sophie Germann  
Berend Snijder · Paul Fransz · Valérie Gaudin

## The *Arabidopsis* LHP1 protein is a component of euchromatin

Received: 11 June 2005 / Accepted: 29 August 2005 / Published online: 22 October 2005  
© Springer-Verlag 2005

**Abstract** The HP1 family proteins are involved in several aspects of chromatin function and regulation in *Drosophila*, mammals and the fission yeast. Here we investigate the localization of LHP1, the unique *Arabidopsis thaliana* HP1 homolog known at present time, to approach its function. A functional LHP1–GFP fusion protein, able to restore the wild-type phenotype in the *lhp1* mutant, was used to analyze the subnuclear distribution of LHP1 in both *A. thaliana* and *Nicotiana tabacum*. In *A. thaliana* interphase nuclei, LHP1 was predominantly located outside the heterochromatic chromocenters. No major aberrations were observed in heterochromatin content or chromocenter organization in *lhp1* plants. These data indicate that LHP1 is mainly involved in euchromatin organization in *A. thaliana*. In tobacco BY-2 cells, the LHP1 distribution, although in foci, slightly differed suggesting that LHP1 localization is determined by the underlying genome organization of plant species. Truncated LHP1 proteins expressed in vivo allowed us to determine the function of the different segments in the localization. The in foci distribution is dependent on the presence of the two chromo domains, whereas the hinge region has some nucleolus-targeting properties. Furthermore, like the animal HP1 $\beta$  and HP1 $\gamma$  subtypes, LHP1 dissociates from chromosomes during mitosis. In transgenic plants expressing the LHP1–GFP fusion protein, two major localization patterns were observed according to cell types suggesting that localization evolves with age or differentiation states. Our results show conversed characteristics of the

*A. thaliana* HP1 homolog with the mammal HP1 $\gamma$  isoform, besides specific plant properties.

**Keywords** *Arabidopsis* · Chromatin · Heterochromatin protein 1 · Mitosis · Nucleolus

**Abbreviations** PI: Propidium iodide · DAPI: 4',6-diamidino-2-phenylindole · HP1: Heterochromatin protein 1 · CD: Chromo domain · CSD: Chromo shadow domain · HR: Hinge region · RHF: Relative heterochromatin fraction · FISH: Fluorescent in-situ hybridization · NLS: Nuclear localization signal · NoLS: Nucleolar localization signal

### Introduction

Heterochromatin protein 1 (HP1) was originally identified as a non-histone component of heterochromatin associated with position effect variegation control. Since then, HP1-like proteins were identified from fission yeast to *Drosophila* mammals and plants, each organism containing one to three isoforms. The HP1-like family is involved in chromosome condensation and segregation, in telomere organization, in nuclear architecture, in control of development and cell cycle by generating and maintaining a silent chromatin structure (Li et al. 2002; Maison and Almouzni 2004).

This functional diversity arises from the specific and conserved structure of the HP1-like proteins. They are characterized by the presence of two sequence-related modules, the amino-terminal chromo domain (CD) and the carboxy-terminal chromo shadow domain (CSD), separated by a variable intervening “hinge” region (HR). These modules participate in protein–protein interactions and in nucleic acid binding (Li et al. 2002; Maison and Almouzni 2004). Thus HP1-like proteins are molecular adaptors that participate in multiple distinct nucleoprotein complexes with various structural and regulatory functions.

M. Libault · S. Germann · V. Gaudin (✉)  
Laboratoire de Biologie Cellulaire, IJPB, INRA, route de St Cyr,  
78026 Versailles Cedex, France  
E-mail: valerie.gaudin@versailles.inra.fr  
Tel.: +33-1-30833522  
Fax: +33-1-30833099

F. Tessadori · B. Snijder · P. Fransz  
Swammerdam Institute for Life Sciences,  
University of Amsterdam, Kruislaan 318, 1098 Amsterdam,  
The Netherlands

In *Arabidopsis thaliana*, a HP1 homolog, LHP1, was isolated independently in screens for early flowering plants (Gaudin et al. 2001), for alterations of inflorescence morphology (Larsson et al. 1998; Kotake et al. 2003) or for altered leaf glucosinolate levels (Kim et al. 2004). The *lhp1/tfl2/TU8* allelic mutations have pleiotropic effects, and affect flowering time, photoperiod and temperature sensitivity, plant architecture, leaf morphology, inflorescence determinacy and hormone levels (Larsson et al. 1998; Ludwig-Müller et al. 1999, 2000; Gaudin et al. 2001; Kotake et al. 2003; Takada and Goto 2003). Furthermore, LHP1 was shown to interact in vitro with the histone H3 dimethylated at lysine 9 (Jackson et al. 2002), a hallmark of silent chromatin recognized by the CD of HP1 proteins (see references in (Berger and Gaudin 2003)). In vitro interaction between LHP1 and NtSET1, a tobacco histone methyltransferase and their colocalization were also reported (Yu et al. 2004). Taken together, these data suggest that LHP1 plays a role in gene regulation and developmental control by establishing and maintaining specific silent chromatin domains.

On the contrary to *A. thaliana*, where a unique HP1 homolog was recorded in its sequenced genome (Gaudin et al. 2001; ChromDB, <http://chromdb.org/>), mammals have three HP1 isoforms ( $\alpha$ ,  $\beta$ ,  $\gamma$ ). Despite similarities in structure and sequences, the three mammal isoforms have non-redundant functions or even opposite effects on gene regulation as described for HP1 $\alpha$  and HP1 $\gamma$  (Li et al. 2002). These three HP1 subtypes present heterogeneous patterns of nuclear localization and differ in their recruitment to euchromatin and heterochromatin both in interphase and during cell cycle (Yamada et al. 1999; Minc et al. 2001; Sugimoto et al. 2001; Hayakawa et al. 2003). These data highlight various functions for HP1-like proteins and thus question the function of LHP1 in plants. Here we investigate the nature of the LHP1-associated chromatin domains for the purpose of better understanding the LHP1 function.

We have analyzed the subnuclear distribution of LHP1 in *A. thaliana* and *Nicotiana tabacum*, two species characterized by different genome sizes and different heterochromatin contents. The impact of the *lhp1* mutation on the nuclear organization was studied. Furthermore, the dynamics of the LHP1 distribution was analyzed throughout the cell cycle and development. These data highlight some aspects of the LHP1 function in plants compared to animals.

## Materials and methods

### Plant materials

The *lhp1-1* and *lhp1-2* mutants were isolated from the Versailles T-DNA insertion collection of *A. thaliana* (Gaudin et al. 2001). For flowering time analyses, plants were grown in growth chambers under short-day (SD; 8-h light/16-h dark, with alternate 20°C/16°C tempera-

tures), or long-day (LD; 16-h light/8-h dark, at 20°C constant temperature) conditions. The *N. tabacum* L. cv. Bright Yellow 2 (tobacco BY-2 or TBY-2) cell line was obtained from C. Bergounioux (IBP, Orsay, France). The cell line was grown in the dark, at 24°C, under constant shaking and maintained by weekly subcultures (Nagata et al. 1992).

### TBY-2 cell synchronization and mitotic events

For synchronization, 4 ml of stationary phase cell culture was transferred to 40 ml fresh medium supplemented by 2  $\mu$ g/ml aphidicolin (Sigma) (Planchais et al. 1997). After 24 h at 24°C, aphidicolin was removed by centrifugation, the pelleted cells were washed and resuspended in fresh medium. The mitotic peak could be observed at 9–10 h after the aphidicolin release. To obtain a highly synchronized cell population starting at the M phase, the aphidicolin-treated cells were subsequently cultivated with 1.6  $\mu$ g/ml propyzamide (Sigma) for at least 10 h before analysis. The second inhibitor was removed by centrifugation and two additional washes. Mitosis was visualized with DRAQ5<sup>TM</sup> (Biostatus).

### Nuclease assay

To prepare nuclei, 5 g of seedlings was ground in a prechilled mortar on ice, with 20 ml of cold nuclei isolation buffer [NIB: 10 mM Tris-HCl pH 7.5, 0.7 M sorbitol, 5 mM MgCl<sub>2</sub>, 5 mM  $\beta$ -mercaptoethanol, 1 mM Pefabloc<sup>®</sup> SC (Pentapharm, Basel, Switzerland)]. After filtration through a nylon mesh, the filtrate was centrifuged (10 min, 200 g, 4°C). The nuclei were washed twice and resuspended in NIB. The quality and concentration of the nuclei were checked by staining an aliquot with 30  $\mu$ g/ml Hoechst 33342 [1 vol in 1 vol of 4% paraformaldehyde in 1 $\times$ PBS (137 mM, NaCl, 2.7 mM KCl, 4.3 mM Na<sub>2</sub>HPO<sub>4</sub> 2H<sub>2</sub>O, 1.4 mM KH<sub>2</sub>PO<sub>4</sub>, pH 7.3)] and by observations on an epifluorescence microscope. DNA concentration was estimated after phenol/chloroform DNA extraction, ethanol precipitation, resuspension in water and OD<sub>260</sub> measurement. The nuclei were resuspended in NIB supplemented with 3 mM CaCl<sub>2</sub> to obtain a 0.1  $\mu$ g/ $\mu$ l equivalent DNA concentration. The samples were incubated at 30°C with the *Micrococcus aureus* endonuclease (MNase, Fermentas) (0.25 U/ $\mu$ l final concentration). At various time points, 80  $\mu$ l aliquots were taken, the reaction was stopped by an addition of 329  $\mu$ l of stop solution (150 mM NaCl, 1% SDS, 20 mM EDTA), and incubation 10 min at 37°C. After digestion, nuclei were lysed and incubated with proteinase K (0.5 mg/ml), 30 min at 55°C, then 140  $\mu$ l of 5 M potassium acetate was added. After 15 min on ice, the tubes were centrifuged (15 min, 12,000 g, 4°C). The supernatants were extracted with phenol/chloroform/isoamyl alcohol (24:24:1) and DNA was precipitated. The DNA pellet was resuspended,

treated with RNase A and the MNase digestion products were analyzed in 1.6% agarose gel.

### Construction of the fusion proteins

PCR fragments corresponding to *LHP1* or truncated *LHP1* (*LHPΔ*) coding sequences were amplified using the pFLcbx5 plasmid as template (Gaudin et al. 2001). The following primers were used: LHP1 (aa 1–445), primers LHP01 (5′GAAGATCTTCCATGGCAATGA AAGGGGCAAGTGGT3′) and LHP02 (5′TCAGATCTA CCCATGGAAGGCGTTCGATTGACTT3′); LHPC (aa 162–445), primers LHP03 (5′GAAGATCTT CCATGGGAAAGCCTGGTAGGAAAC3′) and LHP02; LHPNH (aa 1–378), primers LHP01 and LHP04 (5′TCAGATCTACCCATGGACTCAATCTTGGTTT TCTG3′); LHPH (aa 162–378), primers LHP03 and LHP04; LHPCSD (aa 378–445), primers LHP05 (5′GAAGATCTTCCATGGAGGAGTTGGACATCA CG3′) and LHP02; LHPN (aa 1–194), primers LHP01 and LHP06 (5′TCAGATCTACCCATGGACTCA GTAGCATCATGTGA3′). PCR fragments were digested with *NcoI* (underlined restriction site), and inserted at the *NcoI* restriction site of the pAVA121 vector harboring the S65T GFP protein driven by the 35S CaMV promoter (Gaudin et al. 2001). LHP1 and truncated LHP1 proteins were fused to the N-terminal region of the GFP. The bipartite NLS of the VirD2 protein was fused to the C-terminal end of the LHPCSD–GFP fusion (Gaudin et al. 2001). Sequencing was performed to verify the constructs. The 35S::LHPΔ–GFP constructs were introduced into the pCambia1300 binary vector ([http://www.cambia.org/pCAMBIA\\_vectors.html](http://www.cambia.org/pCAMBIA_vectors.html)), transferred into the GV3101 (pMP90) *Agrobacterium tumefaciens* strain. *Arabidopsis* transformations were performed as in Gaudin et al. (2001).

### *Agrobacterium* transformation

*A. thaliana in planta* transformations were performed and transgenic plants were selected as described by Gaudin et al. (2001). The establishment of stable TBV-2 transgenic cell lines was carried out as described by Trehin et al. (1997). Independent calli were obtained, transferred to liquid medium and maintained by weekly subcultures.

### Heterochromatin content quantification and FISH analysis

The relative heterochromatin fraction (RHF) was established by determining the fluorescence of all chromocenters relative to the fluorescence intensity of the entire nucleus (Soppe et al. 2002). Fluorescence in-situ hybridizations (FISH) experiments were carried out as described in Fransz et al. (1998). The following probes were used: pAL1, containing the centromeric 180 bp, the

pericentromeric 5S rDNA (Fransz et al. 1998) and 45S rDNA (Gerlach and Bedbrook 1979).

### Staining and fluorescence observations

Cell walls were visualized after incubating in a propidium iodide (PI) solution (5 μg/ml). According to tissues and species, various DNA-specific fluorescent dyes were used: DAPI (4′,6-diamidino-2-phenylindole), Hoechst 33342 or DRAQ5™. For coupled detections of DAPI and GFP, *A. thaliana* tissues were gently fixed in 4% paraformaldehyde in PBS for 2 min and incubated with a DAPI solution (10 μg/ml) for 30–50 min. Methylated DNA was detected using anti-5methyl-cytosine (Eurogentec) as described previously (Soppe et al. 2002). To visualize DNA content of TBV-2 cells, cells were incubated in 80 μg/ml of Hoechst 33342 solution without fixation. PI and GFP fluorescence observations were performed on a LEICA TCS-NT laser scanning confocal microscope (Leica Microsystems, Heidelberg, Germany) as previously described (Gaudin et al. 2001) and DAPI/GFP observations on a LEICA TCS-SP2 spectral confocal microscope equipped with AOTF for excitation, with a water-cooled argon-UV laser (351 and 364 nm, Spectra-Physics 2020–05), and with an air-cooled argon-visible laser (488 nm). Observations were realized with a BP340–380/LP425 filter for DAPI and with a BP460–500/BP512–542 for GFP. The public ImageJ software (NIH, USA) was used to analyze DAPI and GFP fluorescence intensity profiles. Representative images were chosen to illustrate the observations.

### RT-PCR analyses

Total RNAs were prepared from seedling using the TRIzol reagent (Life Technologies). 1–2 μg of DNase treated total RNAs were used to perform RT-PCR (Gaudin et al. 2001) with oligonucleotides Mav11 (5′GAGGAGTTGGACATCACGAAG3′) and GFP4 (5′TGACTTCAGCACGTGTCTTG3′), specific for the LHP1–GFP fusion. 28–32 cycles were used. The number of cycles chosen was shown to be in the linear range of the reaction in a separated experiment using different amounts of cDNA template. Two biological and three technical repetitions were analyzed. The amplified PCR products were separated on an agarose gel and quantified using a GelDoc 1000 (BioRad) imaging system. The level of expression of the adenine phosphorybosyl transferase (*APT1*) was measured in each sample and used to normalize the results (Gaudin et al. 2001).

## Results

### Expression of a LHP1–GFP fusion protein is able to rescue the *lhp1* mutation

Previous experiments in tobacco protoplasts have shown a nuclear localization of LHP1–GFP fusion protein with

a specific foci distribution (Gaudin et al. 2001). These preliminary observations were realized after transient expression in a heterologous system. To further investigate the subnuclear localization of LHP1 *in planta*, we stably introduced a LHP1–GFP fusion construct into *A. thaliana* wild-type and *lhp1-1* mutant plants. Several independent transgenic lines (lhpLG) were obtained, of which six lines were further analyzed. Based on plant morphology and architecture, three phenotypic groups could be identified (Fig. 1). The transgenic plants in the first group (lhpLG1–3), had similar phenotype to *lhp1-1* (early flowering and dwarf plants with a curled leaf phenotype) or an even more affected phenotype (lhpLG1, smaller plants than *lhp1-1* with very curled leaves). The second group (lhpLG4) contained plants with an intermediary phenotype, while in the third one (lhpLG5–6), restoration of a normal rosette and leaf phenotypes was observed. Flowering time phenotypes of the transgenic plants were recorded (Table 1), and revealed partial restoration especially in SD. The *lhp1* mutant phenotype being very pleiotropic, the degree of restoration slightly varied according to observed phenotypic traits. The level of expression of the *LHP1–GFP* transgene was recorded by semi-quantitative RT-PCR for each line and the data showed a good correlation between the phenotype and the level of transgene expression (data not shown). Plants with normal rosettes (lhpLG4–6) showed a high level of *LHP1–GFP* expression (one- to threefold the expression level of *APT1*, a constitutive gene), whereas a low level of expression was found in plants with the mutant phenotype (lhpLG1–3).

The *LHP1–GFP* expression of the first and third groups differed by a factor 6–13. Therefore, we conclude that the LHP1–GFP fusion is functional *in planta*, being able to restore most of the pleiotropic traits of the *lhp1* mutant such as leaf morphology and plant architecture. Wild-type plants were also transformed with the 35S::LHP1–GFP construct (WtLG plants) and did not show any peculiar phenotype (Fig. 1).

Distribution of LHP1–GFP and chromatin organization in the *lhp1* mutants imply a predominant euchromatic function of LHP1

LHP1 localization studies were performed in both WtLG1 and lhpLG5 transgenic lines, both of which have a phenotype close to normal. Similar GFP fluorescence patterns were observed in the two lines (data not shown). A fluorescent nucleoplasm with small fluorescent foci was observed with exclusion from the nucleolus (Fig. 2). To determine the nature of the LHP1 foci, the GFP and DAPI fluorescent patterns were compared (Fig. 2). Line-scan analysis generally revealed no overlap of the LHP1–GFP signals with DAPI-bright chromocenters. These are known to be the nuclear domains of heterochromatin in *A. thaliana* (Fransz et al. 1998, 2002). Partial overlap between GFP-LHP1 and chromocenters was observed in less than 10% of the cases. These data suggest that LHP1 is mainly associated with the euchromatic fraction.

**Fig. 1 a–f** Transgenic *A. thaliana* plants bearing the LHP1–GFP fusion protein (LG). Rosettes of 3-week-old plants, cultivated in LD conditions, visualized at the same magnification. **a** Wild-type plant; **b** WtLG1; **c** *lhp1-1* mutant plant; **d–f** lhpLG1, 4 and 5, respectively

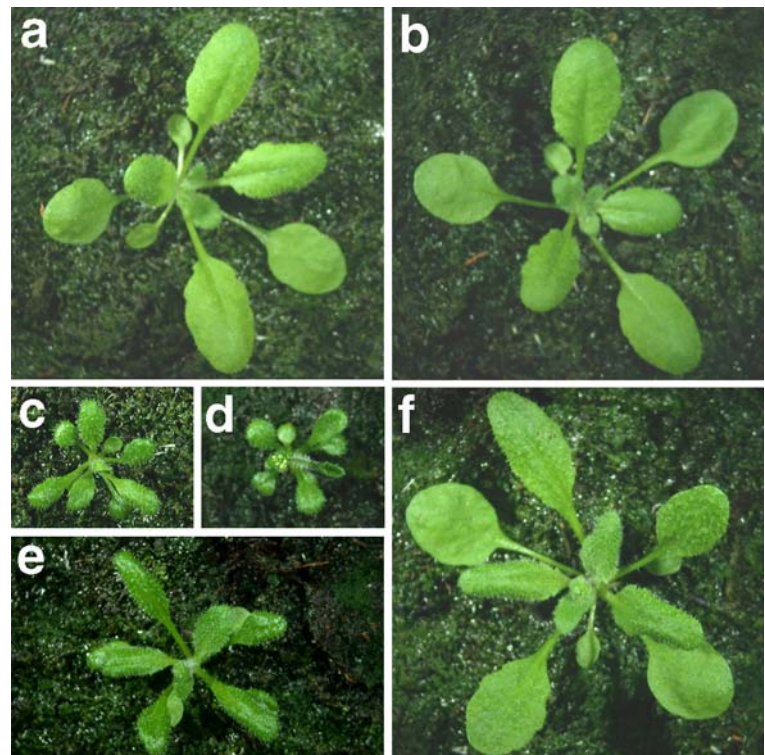


**Table 1** Flowering responses of *A. thaliana* LG transgenic plants. Plants were grown under short-day (SD) or long-day (LD) conditions. Flowering time (FT) expressed in days from sowing to the appearance of a 0.2-cm stem and numbers of rosette leaves (RL) were recorded on 6–10 plants.  $\pm$  Standard deviation

	In SD		In LD	
	FT	RL	FT	RL
Wt	60.5 $\pm$ 1.6	53.9 $\pm$ 3.4	25.5 $\pm$ 0.8	10 $\pm$ 0.5
lhp1-1	39.5 $\pm$ 1.7	14.6 $\pm$ 0.7	20.6 $\pm$ 0.9	7.9 $\pm$ 0.6
WtLG1	66.8 $\pm$ 2.1	55.8 $\pm$ 6.5	24.4 $\pm$ 1.4	9.4 $\pm$ 1.1
WtLG2	66.7 $\pm$ 4.8	47.3 $\pm$ 8.6	24.0 $\pm$ 0.9	9.1 $\pm$ 0.6
WtLG3	64.6 $\pm$ 3.2	51.6 $\pm$ 11.9	24.4 $\pm$ 1.8	9.5 $\pm$ 1.1
lhpLG1	37.1 $\pm$ 1.2	11.9 $\pm$ 0.6	18.3 $\pm$ 0.5	6.3 $\pm$ 0.5
lhpLG2	36.1 $\pm$ 2.2	11.6 $\pm$ 1.1	18.9 $\pm$ 0.6	6.6 $\pm$ 0.7
lhpLG3	38.0 $\pm$ 2.3	12.0 $\pm$ 0.9	18.2 $\pm$ 0.4	6.2 $\pm$ 0.4
lhpLG4	42.1 $\pm$ 2.3	17.4 $\pm$ 1.1	21.2 $\pm$ 0.8	7.9 $\pm$ 0.7
lhpLG5	44.8 $\pm$ 4.3	17.6 $\pm$ 0.9	22.0 $\pm$ 0.8	8.5 $\pm$ 0.9
lhpLG6	51.8 $\pm$ 1.7	18.4 $\pm$ 2.1	22.1 $\pm$ 1.1	8.5 $\pm$ 0.5

To define whether LHP1 has impacts on chromatin organization, we examined the heterochromatin content in wild-type and *lhp1* mutant nuclei. DAPI staining was performed on *lhp1-1*, *lhp1-2* and wild-type nuclei isolated from different organs and the heterochromatin fraction was determined (Fransz et al. 1998; Soppe et al. 2002). To minimize the developmental

differences between the wild-type plant and the *lhp1* mutant, which flowers earlier than the wild type, we examined nuclei from sepals and petals isolated at the same developmental stage. The shape, size or number of chromocenters did not significantly differ between *lhp1* and wild-type nuclei (Fig. 3) neither did the relative heterochromatic fractions (RHF; Fig. 3c). In rosette leaves, the RHF slightly varied in wild-type plants during the analyzed developmental window and to a lower extent in the mutants. This could suggest a minor role for LHP1 in heterochromatin formation during development or cell differentiation. To test a further role of LHP1 in the organization of heterochromatic chromocenters, FISH experiments were carried out using the centromeric 180-pb repeat, 5S rDNA pericentromeric and 45S rDNA probes. The corresponding genomic sequences were previously shown in chromocenters (Fransz et al. 2002). No major differences in their organization could be observed between mutant and wild-type plants (Fig. 3d, g).

To examine if the *lhp1* mutation affects chromatin condensation, treatments with the *Micrococcus aureus* MNase were performed on wild-type and *lhp1* mutant nuclei (Fig. 4). At a global level, chromatin of *lhp1* nuclei was more rapidly digested than wild-type chromatin, suggesting a higher accessibility to nucleases and consequently, a lower compaction level. As

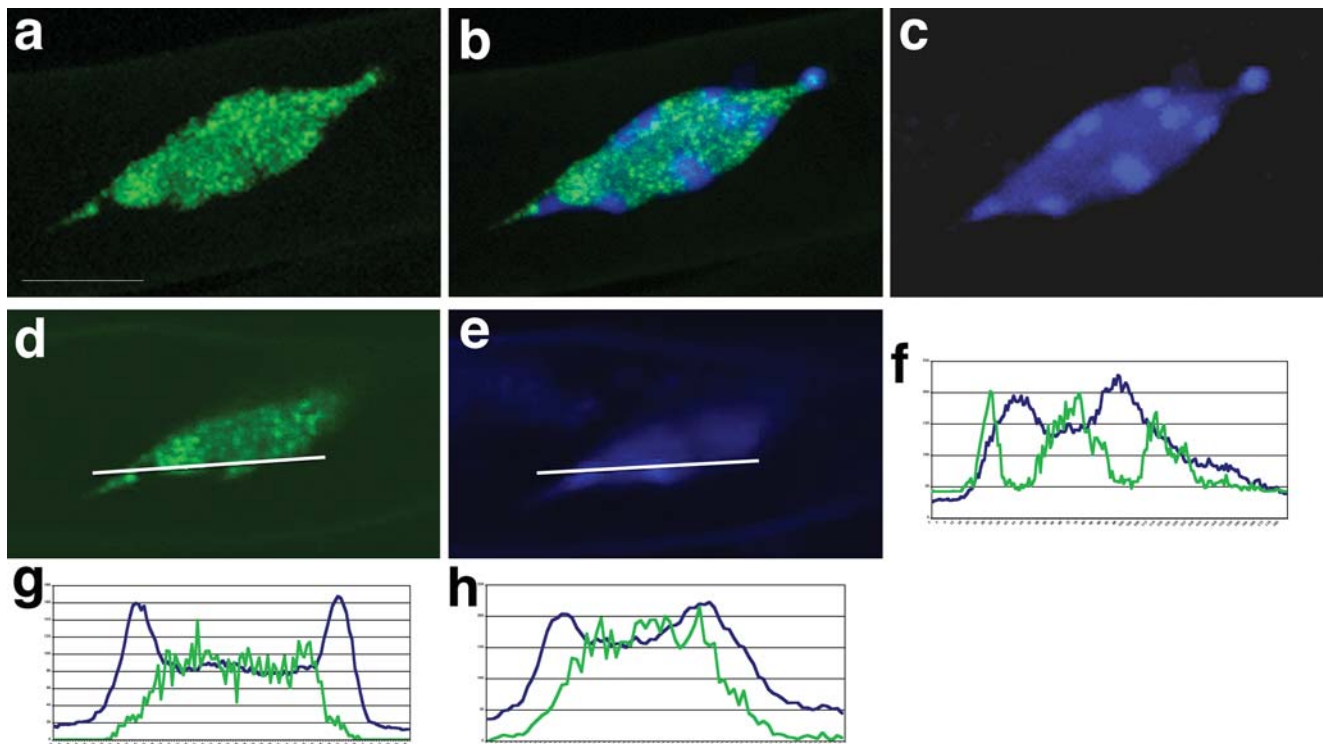


**Fig. 2** Localization of LHP1-GFP in the transgenic *A. thaliana* lhpLG5 line. Confocal projections of a root hair nucleus. **a** GFP fluorescence; **b** overlay; **c** DAPI coloration; a section throughout the nucleus was analyzed using the ImageJ software; **d** GFP and

DAPI fluorescences; **f** profiles of GFP (green) and DAPI (blue) fluorescence intensities on the white line; profiles throughout a guard cell nucleus (**g**) and an epicotyl cell nucleus (**h**). Scale bar: 10  $\mu$ m

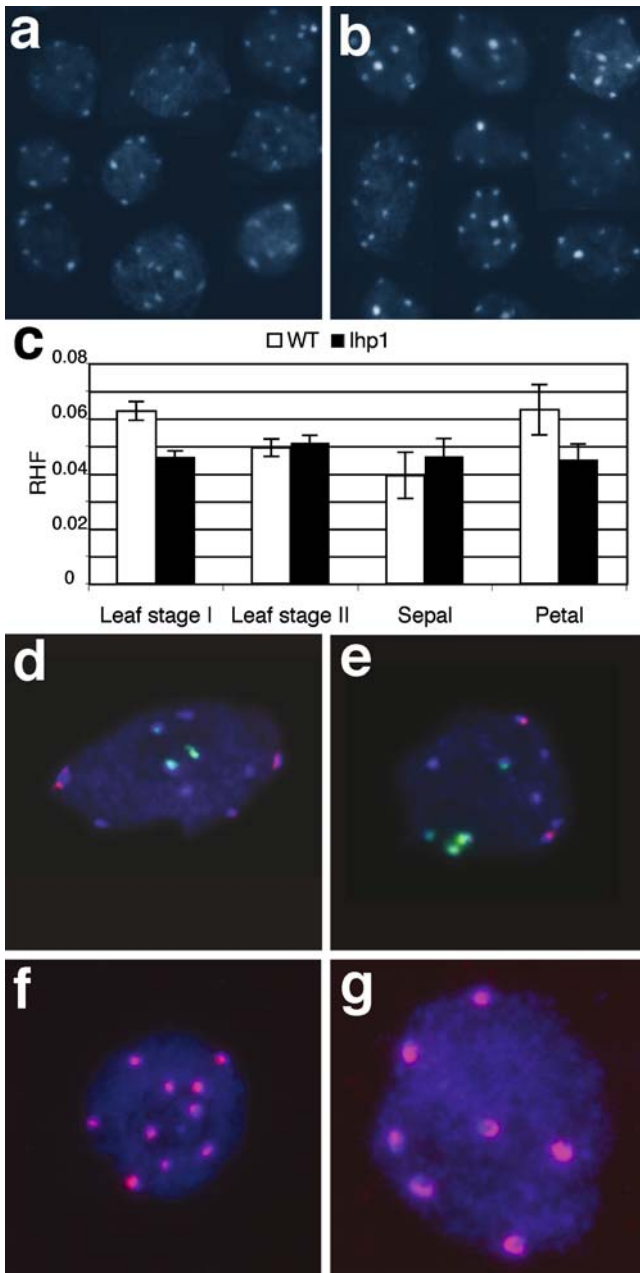


**Fig. 3 a–g** Heterochromatin organization. Phenotypes of *A. thaliana* wild-type (**a**) and *lhp1-1* (**b**) nuclei isolated from petals and stained with DAPI. **c** Relative heterochromatin fraction (RHF) in wild-type and *lhp1* nuclei isolated from leaves, sepals and petals. Leaves were isolated from 12-day-old (stage I) and 17-day-old (stage II) rosettes. **d–g** Fluorescence in-situ hybridizations performed to compare the structure of the chromocenters in wild-type and *lhp1* mutant plants. Wild-type (**d, f**) and *lhp1* nuclei (**e, g**) were isolated from rosette leaves. Pericentromeric (red) and rDNA (green) probes (**d–e**) or the 180-bp centromere repeat probe (red, **f–g**) were used. Nuclei were counterstained with DAPI. Scale bar: 10  $\mu$ m

heterochromatin represents only a reduced fraction of the *A. thaliana* genome (10–15%), these significant differences are likely to concern the euchromatic fraction of the genome.

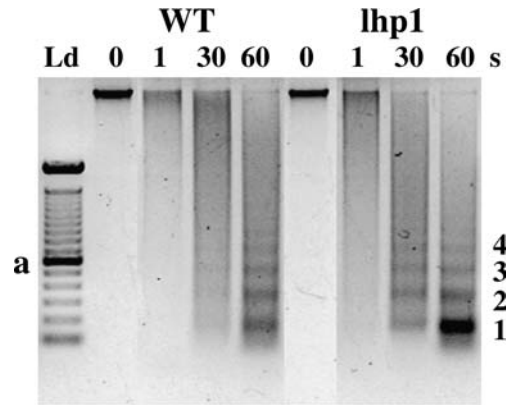


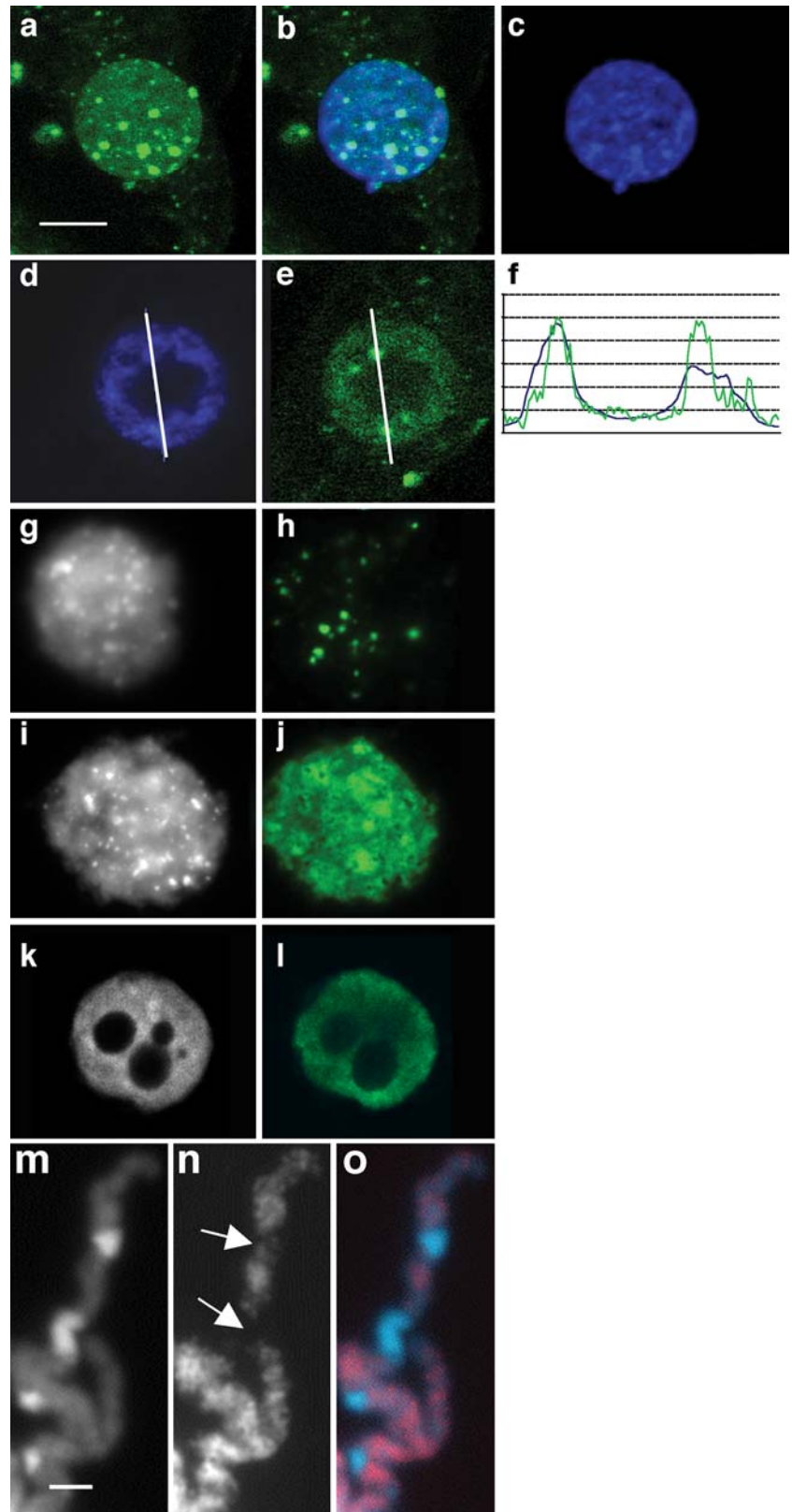
**Fig. 4** Chromatin accessibility assessed by sensitivity to MNase digestion on wild-type and *lhp1* nuclei. Nuclei were treated with MNase (0–60 s). After DNA extraction, the digestion products were analyzed by electrophoresis. A ladder of polynucleosomes is observed after 30 s on the *lhp1* nuclei (1: mononucleosome, 2: dinucleosomes...). Ld: 100 bp DNA Ladder, a: 600-bp fragment

#### Influence of the size of the genome on the LHP1 localization

To test whether the genome organization has effects on the LHP1–GFP localization and whether LHP1 function may diverge in different species, the fusion protein was introduced into *N. tabacum*, which has a genome 45 times larger than the *A. thaliana* genome. Several independent transgenic tobacco TBY-2 cell lines expressing the LHP1–GFP fusion protein were generated and analyzed. All transgenic lines presented the same localization pattern (data not shown). The LHP1–GFP fusion protein was visible in the nucleus as bright GFP–fluorescent foci dispersed in a fluorescent nucleoplasm, but excluded from the nucleolus (Fig. 5a–f). In TBY-2 nuclei, intense DAPI-stained regions have been distinguished, although these regions were less precisely defined and more diffused than the DAPI-stained chromocenters in *A. thaliana*. Combined GFP and DAPI fluorescence detection as well as line-scan analysis of the superimposed images revealed that most of the GFP–fluorescent foci overlapped with DAPI-stained domains (Fig. 5).

To better understand the GFP–LHP1 distribution in tobacco, we investigated the nature of DAPI-stained regions in TBY-2 by FISH experiments and immunolabeling experiments using antibodies against two hallmarks of silent chromatin, the 5-methyl cytosine (5mC) and methylated histone H3 at lysine position 9 (H3K9m; Fig. 5g–l). By using a 45S ribosomal DNA repeat probe, specific of the NOR regions, we showed that DAPI-stained regions did not overlap with the NOR regions. The 5mC labeling was distributed in the whole nucleoplasm with exclusion of brightly stained foci. In metaphase chromosomes these 5mC-empty segments may correspond very well with AT-rich regions (Fig. 5m–o). The presence of large DAPI-positive AT-rich segments in tobacco and other plant species is

**Fig. 5 a–o** Nuclear localization of the LHP1–GFP fusion protein in transgenic *TBY-2* cell lines and nuclear phenotypes of *TBY-2* cells. **a–e** Transgenic *TBY-2* cells expressing LHP1–GFP (LG) and counterstained with DAPI. Confocal projections of the same nucleus showing GFP-fluorescence (**a**), DAPI-fluorescence (**c**) and merged (**b**) images. Corresponding sections (**d**, **e**) and line-scan profile (**f**) on the same nucleus. **g–o** Nuclei or chromosomes of wild-type *TBY-2* cells. **g**, **h** FISH experiments with 45S rDNA probe (**h**) and DAPI counterstaining (**g**). **i**, **j** Immunolabeling using 5mC antibody (**j**) and DAPI counterstaining (**i**). **k**, **l** Immunolabeling using H3K9m antibody (**l**) and DAPI counterstaining (**k**). **m–o** Microscope images showing mitotic chromosomes of *TBY-2* cells after immunolabeling with anti-5mC (**n**) and counterstained with DAPI (**m**). The *arrows* indicate the positions of DAPI-positive segments, which are presumed to be AT-rich. If so, then these segments contain little GC pairs and are hardly stained by anti-5mC. DAPI (**m**), 5mC labeling (**n**) and merged (**o**) images. Scale bars **a–l**: 10  $\mu$ m, **m–o**: 3  $\mu$ m



known from several studies (Moscone et al. 1996; Ali et al. 2000; Liu et al. 2004). However, such large AT-rich segments are not present in the *A. thaliana* genome.

Consistent with this observation, the H3K9m distribution was also uniform throughout the nucleus with exclusion from the nucleolar regions. These results

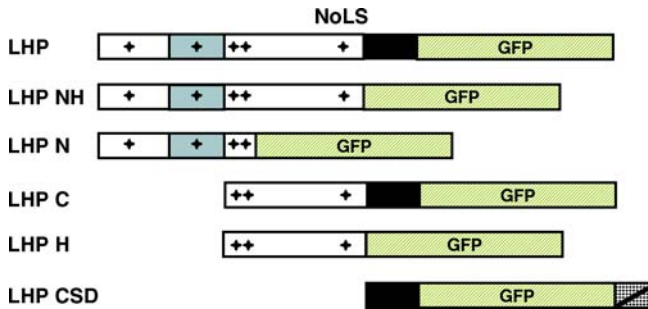


**Fig. 6** Schematic representations of LHP1 and truncated LHP1 proteins fused to GFP. LHPNH: N-terminal and hinge regions (aa 1–378). LHPN: N-terminal region (aa 1–194). LHP C: long C-terminal region (aa 162–445). LHPH: hinge region (aa 162–378). LHPCSD: short C-terminal region (aa 378–445). The *gray*, *black* and *hatched boxes* represent the chromo domain, the chromo shadow domain and the VirD2 NLS region, respectively. The *stars* indicate the positions of the five LHP1 classical nuclear localization signals (NLS1–5). NLS3 and NLS4 form a bipartite signal. NLS5 may participate in a putative nucleolar-targeting signal (NoLS)

suggest that in tobacco, no particularly enriched regions in the H3K9m or 5mC can be distinguished. Chromatin associated with these two epigenetic marks is spread in the whole nucleus and no discrete heterochromatic regions, such as the *A. thaliana* chromocenters, can be distinguished.

#### Effects of the LHP1 structural domains on the subnuclear localization

To examine the role of the structural subdomains of LHP1 in the nuclear localization of the protein, truncated LHP1 proteins, including various combinations of the CD, the CSD and the HR, were fused to GFP (Fig. 6). As the LHPCSD region lacks a nuclear localization signal (NLS), the functional bipartite NLS signal of the *A. tumefaciens* VirD2 protein was fused to the carboxy-terminal region of the LHPCSD–GFP protein (Fig. 6). Deletion constructs were introduced into the tobacco TBY-2 cell line. For each construct, the different transgenic lines gave similar patterns. Localization was also analyzed in *Arabidopsis* protoplasts in transient expression (data not shown).

All truncated LHP1 proteins fused to GFP were targeted to the nucleus indicating that at least three out of the five classical NLS are functional in LHP1 both in *N. tabacum* and *A. thaliana* (Fig. 7b–f). NLS3 and NLS4, which form a classical bipartite NLS, were present in all constructs (except LHPCSD) and may be the major NLS. When LHPN, LHPNH or LHPCSD were fused to GFP, a fluorescence distribution was observed throughout the nucleus with nucleolar exclusion and a variable number of foci (Fig. 7b–d). In *N. tabacum* removal of one of the CDs or CSD resulted in smaller and less numerous foci, whereas in *A. thaliana* foci disappeared

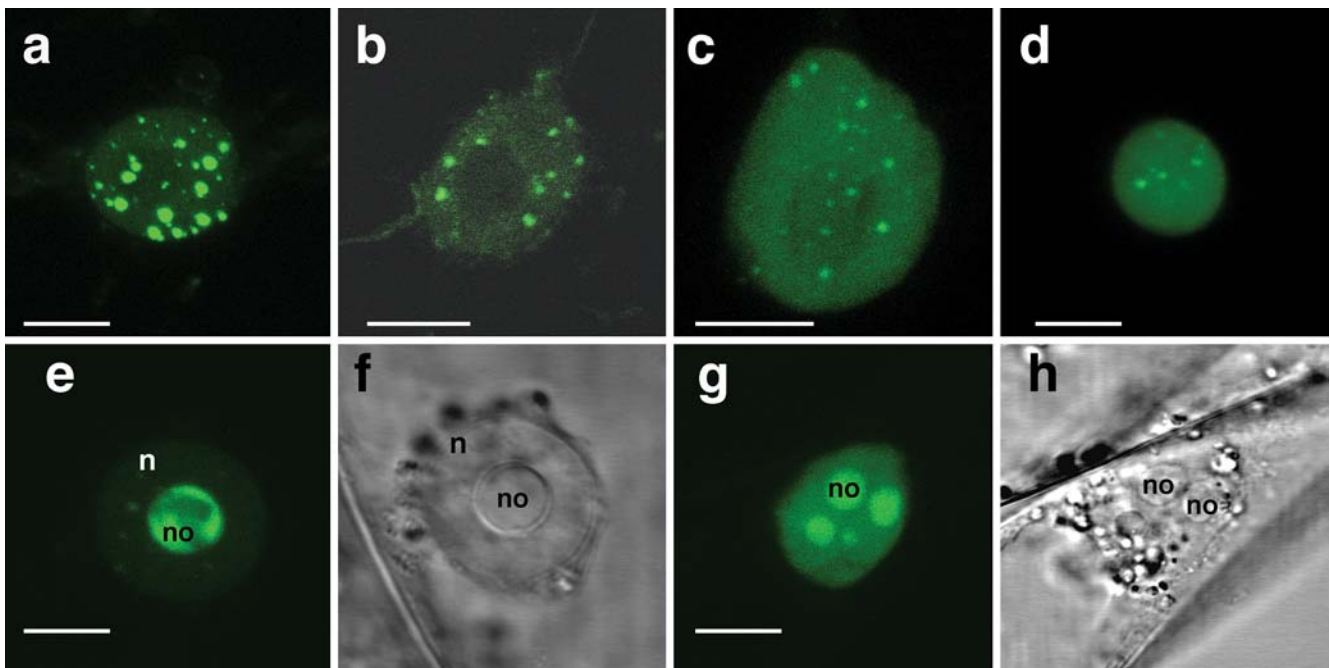


**Fig. 7** a–h Nuclear localization of truncated LHP1 fusion proteins in transgenic TBY-2 cell lines. **a** A transgenic TBY-2 cell expressing the LHP1–GFP (LG) fusion protein (confocal projection of the nucleus). **b–h** LHP1Δ proteins fused to GFP. **b** LHPCSD: projection. **c** LHPNH: projection. **d** LHPN: projection. LHP C: projection (**e**) and light image (**f**), the GFP fluorescence in the

nucleoplasm is very weak, whereas it is strong and non-uniform in the nucleolus. **g** LHPH: projection and corresponding nucleus under light (**h**) of a nucleus presenting a fragmented nucleolus (4 regions) more strongly fluorescent than the surrounding nucleoplasm. *n* nucleoplasm. *no* nucleolus. Scale bars B–S: 10 μm

(data not shown). These data may result from the properties of the CD in recognition of chromatin hallmarks and dimerisation property associated with the CSD (Gaudin et al. 2001). Thus, the CD and CSD have appeared in plants as the main domains involved in foci formation. Both chromodomains were required in *A. thaliana* protoplasts, whereas in *N. tabacum* cells, some foci still can be observed with one of them.

Interestingly, as shown in Fig. 7e–h, respectively, the LHP1C–GFP or LPH–GFP fusions, which both contain the HR, were targeted to the nucleolus, whereas the entire LHP1 protein or the three other constructs were mainly excluded from that nuclear compartment (Fig. 7a–d) both in *A. thaliana* and in *N. tabacum*. The GFP fluorescence signal in the nucleolus seemed to be more intense with the LHPC construct compared to LPH but the distribution more homogenous with LPH. Sequence comparisons with functionally identified nucleolar localization signals (NoLS) (Schmidt et al. 1995; Rowland and Yoo 2003) suggested the presence of a putative NoLS in the LHP1 HR (<sup>314</sup>KRRKSGSVKRRFKQ<sup>326</sup>), formed by two stretches enriched in lysine and arginine residues (underlined) and flanked by one glutamine (Fig. 8). Thus, either the truncated proteins may simply be stored in that compartment due to the deletion of functional domains or the two deletions may induce conformational changes such as the unmasking of a cryptic NoLS, which could relocate the protein to the nucleolus.

Localization of LHP1 is dynamic throughout development and cell cycle

The *in planta* localization of the LHP1–GFP fusion was analyzed in different tissues and at different developmental stages in *A. thaliana*. Two main patterns were observed according to cell types or tissues. The most common pattern, described above as “in foci” pattern, was observed in cells located in older parts of the root and in most of the differentiated cells of the aerial

vegetative tissues such as hypocotyl, epidermis, guard cells, parenchyma (Fig. 9a, b). The second pattern was a uniform fluorescence distribution throughout the nucleus, but excluded from the nucleolus. This “uniform” pattern was observed in nuclei of young proliferating tissue such as the root apex, young hypocotyls, cotyledon cells from immature seeds and young apical meristematic cells (Fig. 9c–g). Nuclei in older root hairs (closer to the crown area) displayed more foci than those in younger root hairs (closer to the root apex), which tend to have a more uniform pattern (Fig. 9h–k).

Due to the larger chromosome size of tobacco and the high mitotic index of TBV-2 cells, the chromosome association of LHP1–GFP was monitored during mitosis, in the transgenic LHP1–GFP tobacco cell line. To better visualize mitosis events, synchronizations of TBV-2 transgenic lines expressing the LHP1–GFP fusion were performed using a combination of aphidicolin and propizamide (Planchais et al. 1997). During prophase, the foci distribution disappeared progressively, and GFP-fluorescence dropped being hardly visible at metaphase (Fig. 10a, b). Only a very weak fluorescent halo was detected around the metaphase plaque, in the ancient nuclear territory (the confocal detection threshold was highly increased to reveal this halo, whose signal is only slightly higher than the background level) (Fig. 10c). Progressively, a fluorescent signal reappeared concomitant with the segregation of the chromosomes and their decondensation (Fig. 10d–f). From late anaphase to telophase, fluorescent foci reappeared until the classical distribution was observed when nuclei have divided. Similar observations were made in mitotic cells located in *A. thaliana* root apex (Fig. 11).

## Discussion

LHP1 is mainly involved in euchromatin organization

In the recent years, an increasing set of chromatin proteins has been described in the *A. thaliana* model system,

LHP1		KRRK	SGSV	KRFK	Q	DGS
Hdm2–MDM2		KKLLK		KRNK		
S6		KRRR	IAL	KKQR	TKKNK	
PRRSV N	PG	KKNK		KKNP	EKPHFPLAT	
L5	VYE	KKPK	REV	KKKK		
Nucleolin		KRKK	EMANKSAPEA	KKKK	KKHKKKHKE	
pNO40		KRAR	HTSKDSKAAKK	KKKK	KKHKKKHKE	
MEQ		RRRK	RNRDAA	RRRR	RKQ	
Protein VII	RRYAKM	KRRR		RR		
Rev		RQA	RRHR	RRR	RERQR	
Coilin		KKNK		RKNK		

**Fig. 8** The putative LHP1 nucleolar localization signal (NoLS). Sequence alignments with NoLS sequences of MDM2/Hdm2 (Lohrum et al. 2000; Weber et al. 2000), coilin (Hebert and Matera 2000), nucleolin (Schmidt-Zachmann and Nigg 1993), L5 protein (Weber et al. 2000), the human ribosomal protein S6 (Schmidt et al. 1995), the human pNO40 protein (Chang et al. 2003), the PRRSV

N viral protein (Rowland et al. 2003), the Herpesvirus oncoprotein MEQ (Liu et al. 1997), the Adenovirus protein VII (Lee et al. 2003) and the Rev protein from HIV (Cochrane et al. 1990). Two basic stretches are boxed (first one is NLS5). One glutamine (Q) residue flanks the NoLS as observed in some viral NoLS

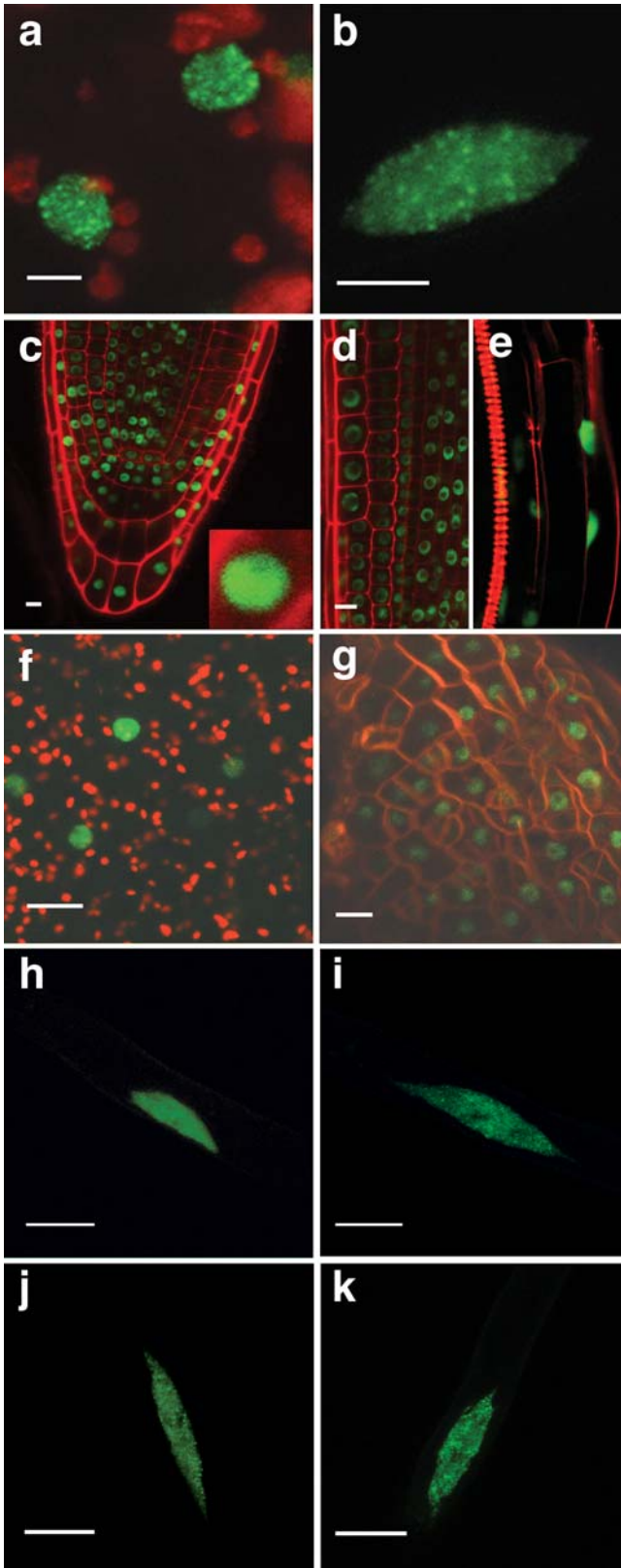


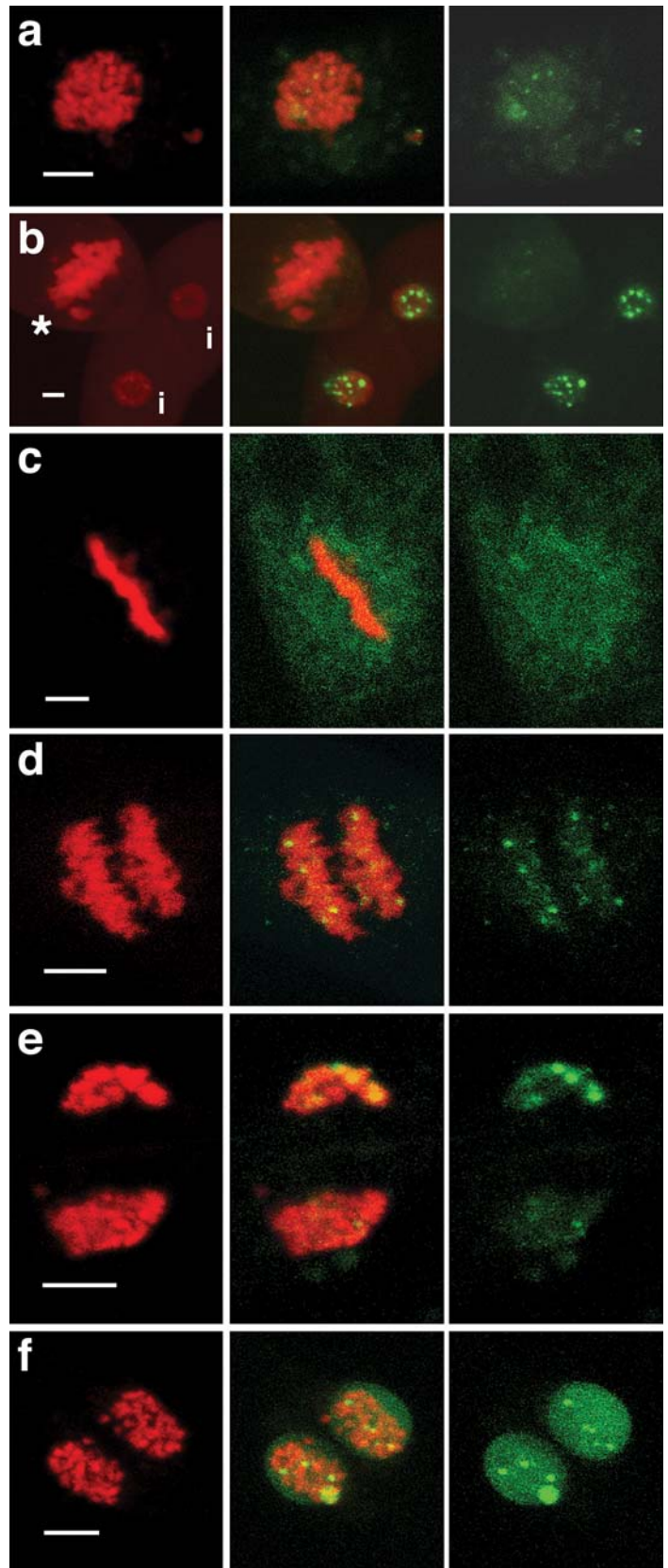
**Fig. 9** Main localization patterns of LHP1-GFP in transgenic *A. thaliana*. “In foci” distribution pattern in a guard cell (a) and a root epidermal cell (b). c–g Uniform distribution pattern in root apex with a closer view of a nucleus with a uniform distribution (c), in cell elongation region (d), close to vascular tissue in the same region (e), in a meristematic cell of the shoot apex (f) and in a cell located in a cotyledon of an immature seed (g). h–k Root hair cell nuclei located from root apex (h) to upper regions (k). The number of foci progressively increased. Scale bars: 10  $\mu$ m

He and Amasino 2005). At a structural and cytological level, *A. thaliana* chromatin is well characterized (Tessadori et al. 2004) and representative of plant chromatin with a small microscopically visible heterochromatin fraction. Thus, heterochromatin in *A. thaliana* nuclei is confined to discrete chromocenters, containing all major repeats and enriched in methylated DNA and H3K9m and corresponding to NOR, centromeric and pericentromeric regions (Fransz et al. 2002; Tessadori et al. 2004). The *A. thaliana* chromocenters are intensely DAPI-stained chromatin regions and contain condensed chromatin that is largely inactive in transcription. Comparative studies between *A. thaliana* and other plant models such as species with higher heterochromatin fractions and more complex chromatin organization, as revealed in this study, will help to broaden our view of plant chromatin diversity and functions. Indeed, structural and biochemical properties of plant heterochromatin are still largely unknown. We therefore investigated the localization of one putative component of heterochromatin, LHP1, a HP1 homolog identified in several developmental screens (Gaudin et al. 2001; Kotake et al. 2003; Kim et al. 2004). HP1 was originally described as a hallmark for heterochromatin in *Drosophila* and later in human and mouse. It may therefore be surprising to demonstrate in this study that LHP1 does not localize in heterochromatin, at a cytological scale. However, another hallmark of heterochromatin in animals, the trimethylated H3K9 residue is also associated with euchromatin in *A. thaliana* (Naumann et al. 2005), suggesting there are some epigenetic markers that plants, or at least *A. thaliana*, have in common with animals, but for different chromatin states.

Using transgenic *A. thaliana* plants expressing a functional LHP1-GFP fusion protein, we clearly observe a speckled localization of LHP1 in euchromatin, outside the chromocenters. Our data suggest that LHP1 has a primary function in euchromatin rather than in heterochromatin, which is supported by recent indirect observations. Indeed, transcriptional analyses revealed ectopic expression of several euchromatic genes in the *lhp1* mutants, whereas genes located in the heterochromatic knob of *A. thaliana* chromosome 4 (Kotake et al. 2003; our unpublished results) or the most of the transposons located in this region were not affected (our unpublished data). Moreover, DNA methylation of centromeric and rDNA repeat sequences or distribution of the dimethylated H3K9 residue was not affected in the *lhp1* mutant (Malagnac et al. 2002; Lindroth et al. 2004;

highlighting the role of plant chromatin dynamics in various processes such as developmental transitions, gene regulation or maintenance of genome integrity (Berger and Gaudin 2003; Tariq and Paszkowski 2004;

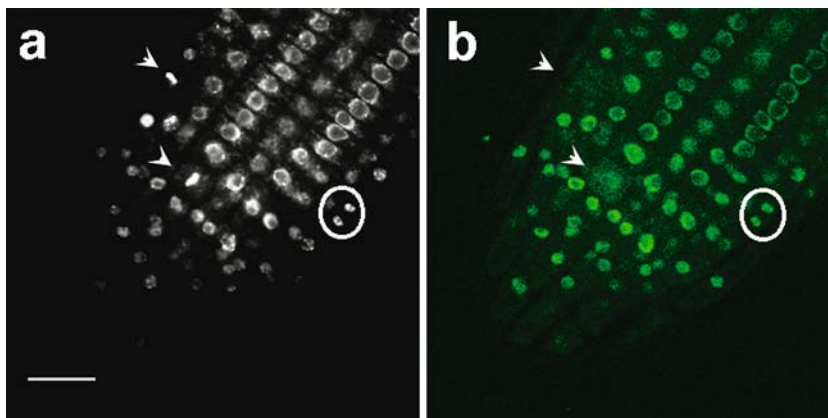
**Fig. 10 a–f** Distribution of the LHP1–GFP fusion protein during mitosis in transgenic tobacco cell lines. DRAQ5™ far red-fluorescence (*left panel*) and GFP-fluorescence (*right panel*). Overlay (*middle panel*). Images are confocal projections. **a** Prophase. **b** A nucleus in late prophase (*asterisk*) and two in interphase (*i*). **c** Metaphase. **d** Anaphase. **e** Telophase. **f** Cytokinesis. Scale bars: 10  $\mu\text{m}$



our unpublished results). We also show here that, in the *lhp1* mutant, the chromocenter organization is not disturbed, whereas global chromatin compaction is

significantly reduced suggesting increased accessibility to euchromatic regions. Altogether, a model can be proposed where LHP1 plays a role in euchromatin structure

**Fig. 11 a, b** Mitotic events in the root apex of an *A. thaliana* transgenic line expressing the LHP1-GFP fusion protein. A section in a root apex viewed on confocal microscope for DAPI (a) and GFP (b) fluorescences. Metaphasic nuclei are indicated by arrows and daughter cells after division by a circle. Scale bar: 20  $\mu$ m



and its absence may lead to a more competent chromatin state for certain sets of euchromatic genes especially genes such as *FT* or floral homeotic genes which are deregulated in the *lhp1* mutants (Gaudin et al. 2001; Kotake et al. 2003; Takada and Goto 2003).

Thus, in agreement with the non-lethal phenotype and the absence of major mitotic defects in the *lhp1* mutants, LHP1 is not a major determinant of heterochromatin in *A. thaliana* as the classical heterochromatic HP1 isoform is in animals. However, in animals HP1-like proteins have wider functions beyond heterochromatin silencing. Indeed, three HP1 isoforms forming the HP1 $\alpha$ ,  $\beta$  and  $\gamma$ -type subfamilies (HP1 $\alpha$ /mHP1 $\alpha$ /HsHP1 $\alpha$ ; HP1 $\beta$ /M31/HsHP1 $\beta$ ; HP1 $\gamma$ /M32/HsHP1 $\gamma$ ; respectively in drosophila, mouse and human) are present in animals. These isoforms exhibit spatially distinct localization patterns and mediate formation of macromolecular chromatin complexes at a range of chromatin sites in euchromatin and/or heterochromatin (Greil et al. 2003). For example, the drosophila HP1 $\gamma$  is restricted exclusively to euchromatin (Smothers and Henikoff 2001) and the mammal HP1 $\gamma$  has a dual localization, both in euchromatin and in heterochromatin (Minc et al. 2001). Furthermore, HP1-like proteins were associated with euchromatic gene regulation to various degrees: HsHP1 $\alpha$  silences genes involved in breast cancer invasion and metastasis HP1 $\alpha$  deposition is directly involved in the repression of two drosophila euchromatic genes in a dose-dependent manner, and of the *cyclin E* gene in human cells, HP1 $\alpha$  and HP1 $\gamma$  interact with repressor complexes, HP1 $\alpha$  can be directly targeted to promoters of *KRAB-KAP-1* repressed genes and HP1 $\gamma$  is associated to repressive complexes regulating E2F and Myc-responsive genes (Kirschmann et al. 2000; Ogawa et al. 2002; see also references in Berger and Gaudin 2003). Although the HP1 $\alpha$ -type subfamily is mainly involved in heterochromatic silencing, the association of the HP1 $\alpha$ -type proteins to heterochromatin and gene silencing may not be so strict. Thus, if locally the two HP1 $\alpha$  and HP1 $\gamma$  subtypes may have similar functions, nuclear cytological data and binding site analyses at large scales highlight a dual function of HP1-like proteins: HP1 $\alpha$  and HP1 $\gamma$  are mainly involved in heterochromatin and euchromatin

structure regulation, respectively (Greil et al. 2003). Thus, based on subnuclear localization, gene regulation and mitosis behavior (see below), the LHP1 is more closely related to the HP1 $\gamma$ -type subfamily although we cannot exclude possible minor roles of LHP1 in heterochromatin.

LHP1 distribution is dynamic throughout the development and cell cycle

Recent studies have shown that HP1 binding is highly dynamic with rapid transient chromatin interaction and exchange, maintaining a stable organization at a higher complexity level (Festenstein et al. 2003; Cheutin et al. 2004; Schmiedeberg et al. 2004). Here we have shown that HP1 distribution is dynamic at a developmental scale. Indeed, the distribution of LHP1-GFP fusion is not identical from cell to cell in the whole plant organism. It varies from a uniform nucleoplasmic distribution in young meristematic cells to a highly punctuated distribution in older tissues. The two main distribution patterns suggest that LHP1 may have different roles throughout plant development and that its distribution pattern is influenced by endogenous factors such as age and differentiation. The age of plant cells being often coupled with polyploidisation, the ploidy level may also influence the LHP1 distribution. Similarly, changes in chromatin composition were described between resting and cycling cells in mammals, among which coupled changes in the histone methylation level and the HP1 $\beta$  distribution (Baxter et al. 2004). These data suggest that LHP1 distribution is a marker of the underlying properties of plant chromatin during development.

The temporal and dynamic redistribution of LHP1 during the plant cell cycle has common features with the HP1 protein behavior during mitosis. In yeast or animals, major delocalization of HP1 occurs as well at the G2/M transition but each subtype seems to have its own specificities (Murzina et al. 1999; Kourmouli et al. 2000; Minc et al. 2001; Sugimoto et al. 2001; Hayakawa et al. 2003; Mateescu et al. 2004). Thus, the LHP1 behavior shares similarities with those of HP1 $\beta$  and HP1 $\gamma$  that

also dissociate from chromosomes during mitosis. Based on similar experiments on HP1 distribution in plant cells during mitosis (Fass et al. 2002), the LHP1–GFP fusion protein is probably delocalized to the cytoplasm during mitosis rather than degraded. The progressive foci reappearance at late anaphase/telophase concomitantly with the beginning of chromosome decondensation and nuclear envelope reformation and interactions of HP1 with nuclear envelope components (Kellum 2003) may suggest a relationship between nuclear envelope and foci reformations.

#### A species-specific LHP1 distribution

The distribution of HP1 subtypes in human, mouse and chicken cells has been demonstrated to be species-specific (Minc et al. 1999; Gilbert et al. 2003). Similarly, the LHP1–GFP foci distribution revealed plant species specificity that may reflect differences in plant genome size and organization. Both in tobacco and *A. thaliana*, LHP1–GFP displays foci indicating specific substructures. However, their position relative to euchromatin and identity is less clear in tobacco compared to *A. thaliana* nuclei. *N. tabacum* is an amphidiploid species with a large genome (approximately 5,730 Mbp,  $n=24$  chromosomes) (Bennett and Leitch 1995), whereas the *A. thaliana* genome is smaller (130 Mbp,  $n=5$  chromosomes). In contrast to *A. thaliana*, the majority of the tobacco nucleus consists of heterochromatin, which does not display chromocenters. Epigenetic markers of visible or large-scale heterochromatin, such as methylated DNA and H3K9m display a dispersed pattern. On the contrary, the H3K4m signal, usually associated with active chromatin, was weak (F. Tessadori, data not shown). These observations underline a predominant heterochromatic interphasic nucleus and the presence of a small euchromatic fraction that is difficult to detect. Similarly, in protoplasts of *N. sylvestris*, one of the diploid parents of *N. tabacum*, the nuclear distribution of dimethylated H3K9 was uniform throughout the nucleus, whereas the dimethylated H3K4 distribution was quite indistinguishable from the H3K9m pattern (Li et al. 2005). These results support a previous study by Houben et al. (2003) who proposed that the absence of H3K4m is a significant mark in defining heterochromatin in large genomes.

#### The LHP1 hinge region has plant-specific features

Analyses of truncated LHP1 proteins expressed in vivo instable transgenic TBY-2 cell lines allowed us to characterize the function of the different segments in the localization. Interestingly, the plant HR, which diverges from the animal HRs, both in size and sequence, may have acquired specific properties. Indeed, we show that the LHP1 HR is targeted to the nucleolus in tobacco cells as well as in *A. thaliana* protoplasts. The animal

HP1 HRs were shown to participate to HP1 targeting (Platero et al. 1995; Smothers and Henikoff 2001), however, such destination was not described. This is possibly due to the delineation of regions for localization analyses or to size and property differences of the HP1 and LHP1 HRs.

The nucleolus is often seen as a storage or sequestration compartment for various proteins. Whether this also occurs for two constructs out of six remains to be solved. Two other possible explanations may account for the observations. Firstly, the whole protein in the other four constructs is present in the nucleolar compartment but the GFP-fluorescence signal may be too faint to be recorded. Secondly, the putative LHP1 NoLS acts in a similar way as cryptic NoLSs, which control the targeting of the MDM2 or coilin proteins to the nucleolus depending on the NoLS accessibility and the protein conformation (Hebert and Matera 2000; Lohrum et al. 2000; Weber et al. 2000). Whether LHP1 may have functions in the nucleolus in certain conditions (post-translational modifications, binding with specific partners...) is an open question. In this context it is interesting to refer to *S. pombe*, where SWI6, the HP1 homolog, represses PolIII-transcribed genes inserted in rDNA clusters (Thon and Verhein-Hansen 2000; Bjerring et al. 2002) or is located in the nucleolus of *clr4* mutants (Ekwall et al. 1996). The unusual nucleolar localization of the LHP1-HR may help to understand the regulatory network, which governs the normal LHP1 localization.

#### The chromodomains are required for the foci formation

By analyzing the localizations of truncated LHP1Δ–GFP fusion proteins, the two chromo domains were shown as the main domains associated with the foci distribution. While both CDs are required for foci localization in *A. thaliana* protoplasts, some foci could be observed with only one CD in *N. tabacum* cells, probably due to the enriched heterochromatic fraction of the tobacco nuclei. These results suggest different subpopulations of foci in plant nuclei corresponding to the underlying genome organization specificities.

In drosophila the exchange of chromo domains between HP1 and Polycomb showed that these domains are responsible for binding to specific chromosomal sites (Platero et al. 1995). Similarly, the LHP1 CD may play a major role in targeting to specific chromatin domains. Analyses of the CD structure and its underlying specificity have shown that it recognizes specific methylated lysine residues (see references in (Brehm et al. 2004)). Although belonging to the same category, the CDs of HP1 and Polycomb present different affinities for the methylated histone marks according to the degree of methylation and the histone H3 tail contexts of the lysine residue (AARK<sup>27</sup>S / QTARK<sup>9</sup>S): the HP1 CD has a higher affinity for the trimethylated H3K9, whereas the Polycomb CD for the trimethylated H3K27 (Fischle

et al. 2003) and the HP1 CD is not able to bind the H3K4m (Jacobs and Khorasanizadeh 2002). The recognition of the specific methylated-lysine mark by the CD of HP1 is mediated by an aromatic cage consisting of three main residues (Tyr, Trp, Tyr/Phe) (Jacobs and Khorasanizadeh 2002; Nielsen et al. 2002). While the first two residues are conserved in LHP1, the third one (Trp 132) is different from its counterpart in HP1 (Tyr 48), but similar to its counterpart (Trp 50) in Polycomb (Fischle et al. 2003). Other critical residues for H3K9m recognition, such as Glu 23, Val 26 and Asp 62 (Jacobs and Khorasanizadeh 2002) or Glu 52 (Tyr 54 in Pc) (Fischle et al. 2003), are replaced in LHP1 by Phe 107 (Val in Pc), Ile 110 (Ala in Pc), Gln 146 and Ala 136, respectively (Gaudin et al. 2001). Although mutagenesis experiment of the Trp 50 residue of Pc into Tyr does not significantly modify the affinity of Pc for H3K27m, the slightly divergent aromatic cage and residues involved in the recognition of H3K9m questions its *in vivo* affinity for methylated histone residues by the LHP1 CD. *In vitro* analyses showed a binding activity of a large N-terminal region of LHP1 (130 aa) including the CD to dimethylated H3K9 (Jackson et al. 2002). Colocalization of LHP1 and H3K9m was recently described in tobacco (Yu et al. 2004). However, methylated H3K9 residue is not an absolute requirement for HP1 binding to chromatin (Cowell et al. 2002) and other marks of the histone code may alone or in a coordinated way, participate to the protein targeting. For example, in *A. thaliana*, at least two coordinated histone modifications, H3K9m and H3K27m, are required *in vitro* for the interaction with the CD of the CMT3 chromomethylase (Lindroth et al. 2004). Thus, LHP1 chromatin recognition may not be exclusive and its CD may binds to several different marks (dimethylated H3K9, methylated H3K27) with different affinities according to the chromatin complex. HP1 has a higher affinity for trimethylated H3K9 and this hallmark, recently associated with euchromatin in *A. thaliana* (Naumann et al. 2005) may also be recognized by LHP1.

As the CSD of LHP1 is involved in the dimerization (Gaudin et al. 2001) and protein–protein interactions (V. Gaudin, unpublished data), it could either target the GFP fusion to regions, where the endogenous tobacco LHP1 proteins are already located (heterodimerisation), or highlight some regions with partners enrichments such as interchromatin granules or nuclear bodies (NBs). Indeed, HP1 was shown to interact with SP100, a component of NBs and colocalizes with them (Hayakawa et al. 2003). Thus, the LHPN–GFP and LHP1CSD–GFP may label different subpopulations of foci, highlighting diverse roles of LHP1 and chromatin interactions. Finally, the tobacco genome may encode several LHP1 subtypes with different specificities such as in animals. Due to the dimerization property and conservation of the CSD, the *A. thaliana* LHP1 may interact with an endogenous HP1-like protein associated with heterochromatin.

Thus, the nature of the foci mediated by the LHP1 CDs as well as the precise histone marks recognized by

the CD of LHP1 and their requirement for LHP1 deposition require further investigation. Due to similarities with HP1 $\gamma$ , foci may correspond to silenced euchromatic regions presenting similarities with Polycomb-silenced regions. Since in some cases both HP1 $\gamma$  and PcG proteins are present in the same complex and contribute to euchromatic gene silencing (Ogawa et al. 2002), the chromatin-silencing mechanism by these two protein types may have more features in common.

**Acknowledgments** ML was supported by a graduate studentship from the French ministry of Research. We thank our colleagues Y. Chupeau and H. Höfte. We are grateful to N. Houba-Herlin, J. Davison and V. Colot (URGV, Evry, France) for critical reading of the manuscript, to O. Grandjean and S. Brown (ISV, Gif/Yvette, France) for confocal analysis support, to C. Bergounioux and C. Perennes (IBP, Orsay, France) for tobacco BY-2 cell lines transformations and W. Bickmore and N. Gilbert (MRC, Edinburgh, U.K.) for advices on MNase protocols.

## References

- Ali HB, Fransz P, Schubert I (2000) Localization of 5S RNA genes on tobacco chromosomes. *Chromosome Res* 8:85–87
- Baxter J, Sauer S, Peters A, John R, Williams R, Caparros ML, Arney K, Otte A, Jenuwein T, Merckenschlager M, Fisher AG (2004) Histone hypomethylation is an indicator of epigenetic plasticity in quiescent lymphocytes. *EMBO J* 23:4462–4472
- Bennett MD, Leitch IL (1995) Nuclear DNA amounts in angiosperms. *Ann Bot* 76:113–176
- Berger F, Gaudin V (2003) Chromatin dynamics and Arabidopsis development. *Chromosome Res* 11:277–304
- Bjerling P, Silverstein RA, Thon G, Caudy A, Grewal S, Ekwall K (2002) Functional divergence between histone deacetylases in fission yeast by distinct cellular localization and *in vivo* specificity. *Mol Cell Biol* 22:2170–2181
- Brehm A, Tufteland KR, Aasland R, Becker PB (2004) The many colours of chromodomains. *Bioessays* 26:133–140
- Chang WL, Lee DC, Leu S, Huang YM, Lu MC, Ouyang P (2003) Molecular characterization of a novel nucleolar protein, pNO40. *Biochem Biophys Res Commun* 307:569–577
- Cheutin T, Gorski SA, May KM, Singh PB, Misteli T (2004) *In vivo* dynamics of Swi6 in yeast: evidence for a stochastic model of heterochromatin. *Mol Cell Biol* 24:3157–3167
- Cochrane AW, Perkins A, Rosen CA (1990) Identification of sequences important in the nucleolar localization of human immunodeficiency virus Rev: relevance of nucleolar localization to function. *J Virol* 64:881–885
- Cowell IG, Aucott R, Mahadevaiah SK, Burgoyne PS, Huskisson N, Bongiorno S, Prantera G, Fanti L, Pimpinelli S, Wu R, Gilbert DM, Shi W, Fundele R, Morrison H, Jeppesen P, Singh PB (2002) Heterochromatin, HP1 and methylation at lysine 9 of histone H3 in animals. *Chromosoma* 111:22–36
- Ekwall K, Nimmo ER, Javerzat JP, Borgstrom B, Egel R, Cranstom G, Allshire R (1996) Mutations in the fission yeast silencing factors *clr4+* and *rik1+* disrupt the localisation of the chromo domain protein Swi6p and impair centromere function. *J Cell Sci* 109:2637–2648
- Fass E, Shahar S, Zhao J, Zemach A, Avivi Y, Grafi G (2002) Phosphorylation of histone h3 at serine 10 cannot account directly for the detachment of human heterochromatin protein 1gamma from mitotic chromosomes in plant cells. *J Biol Chem* 277:30921–30927
- Festenstein R, Pagakis SN, Hiragami K, Lyon D, Verreault A, Sekkali B, Kiuoussis D (2003) Modulation of heterochromatin protein 1 dynamics in primary Mammalian cells. *Science* 299:719–721

- Fischle W, Wang Y, Jacobs SA, Kim Y, Allis CD, Khorasanizadeh S (2003) Molecular basis for the discrimination of repressive methyl-lysine marks in histone H3 by Polycomb and HP1 chromodomains. *Genes Dev* 17:1870–1881
- Franz P, Armstrong S, Alonso-Blanco C, Fischer TC, Torres-Ruiz RA, Jones G (1998) Cytogenetics for the model system *Arabidopsis thaliana*. *Plant J* 13:867–876
- Franz P, De Jong JH, Lysak M, Castiglione MR, Schubert I (2002) Interphase chromosomes in *Arabidopsis* are organized as well defined chromocenters from which euchromatin loops emanate. *Proc Natl Acad Sci USA* 99:14584–14589
- Gaudin V, Libault M, Pouteau S, Juul T, Zhao G, Lefebvre D, Grandjean O (2001) Mutations in *LIKE HETEROCHROMATIN PROTEIN 1* affect flowering time and plant architecture in *Arabidopsis*. *Development* 128:4847–4858
- Gerlach WL, Bedbrook JR (1979) Cloning and characterization of ribosomal RNA genes from wheat and barley. *Nucleic Acids Res* 7:1869–1885
- Gilbert N, Boyle S, Sutherland H, de Las Heras J, Allan J, Jenuwein T, Bickmore WA (2003) Formation of facultative heterochromatin in the absence of HP1. *EMBO J* 22:5540–5550
- Greil F, van der Kraan I, Delrow J, Smothers JF, de Wit E, Bussemaker HJ, van Driel R, Henikoff S, van Steensel B (2003) Distinct HP1 and Su(var)3–9 complexes bind to sets of developmentally coexpressed genes depending on chromosomal location. *Genes Dev* 17:2825–2838
- Hayakawa T, Haraguchi T, Masumoto H, Hiraoka Y (2003) Cell cycle behavior of human HP1 subtypes: distinct molecular domains of HP1 are required for their centromeric localization during interphase and metaphase. *J Cell Sci* 116:3327–3338
- He Y, Amasino RM (2005) Role of chromatin modification in flowering-time control. *Trends Plant Sci* 10:30–35
- Hebert MD, Matera AG (2000) Self-association of coilin reveals a common theme in nuclear body localization. *Mol Biol Cell* 11:4159–4171
- Houben A, Demidov D, Gernand D, Meister A, Leach CR, Schubert I (2003) Methylation of histone H3 in euchromatin of plant chromosomes depends on basic nuclear DNA content. *Plant J* 33:967–973
- Jackson JP, Lindroth AM, Cao X, Jacobsen SE (2002) Control of CpNpG DNA methylation by the KRYPTONITE histone H3 methyltransferase. *Nature* 416:556–560
- Jacobs SA, Khorasanizadeh S (2002) Structure of HP1 chromodomain bound to a lysine 9-methylated histone H3 tail. *Science* 295:2080–2083
- Kellum R (2003) HP1 complexes and heterochromatin assembly. *Curr Top Microbiol Immunol* 274:53–77
- Kim JH, Durrett TP, Last RL, Jander G (2004) Characterization of the *Arabidopsis* *TU8* Glucosinolate Mutation, an allele of *TERMINAL FLOWER2*. *Plant Mol Biol* 54:671–682
- Kirschmann DA, Lininger RA, Gardner LM, Seftor EA, Odero VA, Ainsztein AM, Earnshaw WC, Wallrath LL, Hendrix MJ (2000) Down-regulation of HP1H $\alpha$  expression is associated with the metastatic phenotype in breast cancer. *Cancer Res* 60:3359–3363
- Kotake T, Takada S, Nakahigashi K, Ohto M, Goto K (2003) *Arabidopsis* *TERMINAL FLOWER 2* gene encodes a heterochromatin protein 1 homolog and represses both *FLOWERING LOCUS T* to regulate flowering time and several floral homeotic genes. *Plant Cell Physiol* 44:555–564
- Kourmouli N, Theodoropoulos PA, Dialynas G, Bakou A, Politou AS, Cowell IG, Singh PB, Georgatos SD (2000) Dynamic associations of heterochromatin protein 1 with the nuclear envelope. *EMBO J* 19:6558–6568
- Larsson AS, Landberg K, Meeks-Wagner DR (1998) The *TERMINAL FLOWER2* (*TFL2*) gene controls the reproductive transition and meristem identity in *Arabidopsis thaliana*. *Genetics* 149:597–605
- Lee TW, Blair GE, Matthews DA (2003) Adenovirus core protein VII contains distinct sequences that mediate targeting to the nucleus and nucleolus, and colocalization with human chromosomes. *J Gen Virol* 84:3423–3428
- Li Y, Butenko Y, Graf G (2005) Histone deacetylation is required for progression through mitosis in tobacco cells. *Plant J* 41:346–352
- Li Y, Kirschmann DA, Wallrath LL (2002) Does heterochromatin protein 1 always follow code? *Proc Natl Acad Sci USA* 99(Suppl 4):16462–16469
- Lindroth AM, Shultis D, Jasencakova Z, Fuchs J, Johnson L, Schubert I, Patnaik D, Pradhan S, Goodrich J, Schubert I, Jenuwein T, Khorasanizadeh S, Jacobsen SE (2004) Dual histone H3 methylation marks at lysines 9 and 27 required for interaction with CHROMOMETHYLASE3. *EMBO J* 23:4286–4296
- Liu JL, Lee LF, Ye Y, Qian Z, Kung HJ (1997) Nucleolar and nuclear localization properties of a Herpesvirus bZIP oncoprotein, MEQ. *J Virol* 71:3188–3196
- Liu JY, She CW, Hu ZL, Xiong ZY, Liu LH, Song YC (2004) A new chromosome fluorescence banding technique combining DAPI staining with image analysis in plants. *Chromosoma* 113:16–21
- Lohrum MA, Ashcroft M, Kubbutat MH, Vousden KH (2000) Identification of a cryptic nucleolar-localization signal in MDM2. *Nat Cell Biol* 2:179–181
- Ludwig-Muller J, Krishna P, Forreiter C (2000) A glucosinolate mutant of *Arabidopsis* is thermosensitive and defective in cytosolic Hsp90 expression after heat stress. *Plant Physiol* 123:949–958
- Ludwig-Muller J, Pieper K, Ruppel M, Cohen JD, Epstein E, Kiddle G, Bennett R (1999) Indole glucosinolate and auxin biosynthesis in *Arabidopsis thaliana* (L.) Heynh. glucosinolate mutants and the development of clubroot disease. *Planta* 208:409–419
- Maison C, Almouzni G (2004) HP1 and the dynamics of heterochromatin maintenance. *Nat Rev Mol Cell Biol* 5:296–304
- Malagnac F, Bartee L, Bender J (2002) An *Arabidopsis* SET domain protein required for maintenance but not establishment of DNA methylation. *EMBO J* 21:6842–6852
- Mateescu B, England P, Halgand F, Yaniv M, Muchardt C (2004) Tethering of HP1 proteins to chromatin is relieved by phosphoacetylation of histone H3. *EMBO Rep* 5:490–496
- Minc E, Allory Y, Courvalin JC, Buendia B (2001) Immunolocalization of HP1 proteins in metaphasic mammalian chromosomes. *Methods Cell Sci* 23:171–174
- Minc E, Allory Y, Worman HJ, Courvalin JC, Buendia B (1999) Localization and phosphorylation of HP1 proteins during the cell cycle in mammalian cells. *Chromosoma* 108:220–234
- Moscone EA, Matzke MA, Matzke AJ (1996) The use of combined FISH/GISH in conjunction with DAPI counterstaining to identify chromosomes containing transgene inserts in amphidiploid tobacco. *Chromosoma* 105:231–236
- Murzina N, Verreault A, Laue E, Stillman B (1999) Heterochromatin dynamics in mouse cells: interaction between chromatin assembly factor 1 and HP1 proteins. *Mol Cell* 4:529–540
- Nagata T, Nemoto Y, Hasezawa S (1992) Tobacco BY-2 cell line as the “HeLa” cell in the cell biology of higher plants. *Int Rev Cytol* 132:1–30
- Naumann K, Fischer A, Hofmann I, Krauss V, Phalke S, Irmeler K, Hause G, Aurich AC, Dorn R, Jenuwein T, Reuter G (2005) Pivotal role of AtSUVH2 in heterochromatic histone methylation and gene silencing in *Arabidopsis*. *EMBO J* 24:1418–1429
- Nielsen PR, Nietlispach D, Mott HR, Callaghan J, Bannister A, Kouzarides T, Murzin AG, Murzina NV, Laue ED (2002) Structure of the HP1 chromodomain bound to histone H3 methylated at lysine 9. *Nature* 416:103–107
- Ogawa H, Ishiguro K, Gaubatz S, Livingston DM, Nakatani Y (2002) A complex with chromatin modifiers that occupies E2F- and Myc-responsive genes in G0 cells. *Science* 296:1132–1136
- Planchais S, Glab N, Trehin C, Perennes C, Bureau JM, Meijer L, Bergounioux C (1997) Roscovitine, a novel cyclin-dependent kinase inhibitor, characterizes restriction point and G2/M transition in tobacco BY-2 cell suspension. *Plant J* 12:191–202
- Platero JS, Hartnett T, Eissenberg JC (1995) Functional analysis of the chromo domain of HP1. *EMBO J* 14:3977–3986

- Rowland RR, Schneider P, Fang Y, Wootton S, Yoo D, Benfield DA (2003) Peptide domains involved in the localization of the porcine reproductive and respiratory syndrome virus nucleocapsid protein to the nucleolus. *Virology* 316:135–145
- Rowland RR, Yoo D (2003) Nuclear-cytoplasmic shuttling of PRRSV nucleocapsid protein: a simple case of molecular mimicry or the complex regulation by import, nucleolar localization and nuclear export signal sequences. *Virus Res* 95:23–33
- Schmidt C, Lipsius E, Kruppa J (1995) Nuclear and nucleolar targeting of human ribosomal protein S6. *Mol Biol Cell* 6:1875–1885
- Schmidt-Zachmann MS, Niggs EA (1993) Protein localization to the nucleolus: a search for targeting domains in nucleolin. *J Cell Sci* 105:799–806
- Schmiedeberg L, Weisshart K, Diekmann S, Meyer Zu Hoerste G, Hemmerich P (2004) High- and low-mobility populations of HP1 in heterochromatin of mammalian cells. *Mol Biol Cell* 15:2819–2833
- Smothers JF, Henikoff S (2001) The hinge and chromo shadow domain impart distinct targeting of HP1-like proteins. *Mol Cell Biol* 21:2555–2569
- Soppe WJ, Jasencakova Z, Houben A, Kakutani T, Meister A, Huang MS, Jacobsen SE, Schubert I, Fransz PF (2002) DNA methylation controls histone H3 lysine 9 methylation and heterochromatin assembly in *Arabidopsis*. *EMBO J* 21:6549–6559
- Sugimoto K, Tasaka H, Dotsu M (2001) Molecular behavior in living mitotic cells of human centromere heterochromatin protein HP1 $\alpha$  ectopically expressed as a fusion to red fluorescent protein. *Cell Struct Funct* 26:705–718
- Takada S, Goto K (2003) TERMINAL FLOWER2, an Arabidopsis homolog of HETEROCHROMATIN PROTEIN1, counteracts the activation of *FLOWERING LOCUS T* by CONSTANS in the vascular tissues of leaves to regulate flowering time. *Plant Cell* 15:2856–2865
- Tariq M, Paszkowski J (2004) DNA and histone methylation in plants. *Trends Genet* 20:244–251
- Tessadori F, van Driel R, Fransz P (2004) Cytogenetics as a tool to study gene regulation. *Trends Plant Sci* 9:147–153
- Thon G, Verhein-Hansen J (2000) Four chromo-domain proteins of *Schizosaccharomyces pombe* differentially repress transcription at various chromosomal locations. *Genetics* 155:551–568
- Trehin C, Ahn IO, Perennes C, Couteau F, Lalanne E, Bergounioux C (1997) Cloning of upstream sequences responsible for cell cycle regulation of the *Nicotiana sylvestris* *CycB1;1* gene. *Plant Mol Biol* 35:667–672
- Weber JD, Kuo ML, Bothner B, DiGiammarino EL, Kriwacki RW, Roussel MF, Sherr CJ (2000) Cooperative signals governing ARF-mdm2 interaction and nucleolar localization of the complex. *Mol Cell Biol* 20:2517–2528
- Yamada T, Fukuda R, Himeno M, Sugimoto K (1999) Functional domain structure of human heterochromatin protein HP1Hsz: involvement of internal DNA-binding and C-terminal self-association domains in the formation of discrete dots in interphase nuclei. *J Biochem* 125:832–837
- Yu Y, Dong A, Shen WH (2004) Molecular characterization of the tobacco SET domain protein NtSET1 unravels its role in histone methylation, chromatin binding, and segregation. *Plant J* 40:699–711